Simulation models for household consumption

Costanzo, Giuseppe Tommaso

Publication date:
2011

Document Version
Publisher's PDF, also known as Version of record

STRATEGIC PLATFORM FOR INNOVATION AND RESEARCH IN INTELLIGENT POWER [IPOWER]

Simulation models for household consumption

Category	**Deliverable**
Identifier	**Task WP1-RT4-1K**
Status	**Published**
Version	**1**
Access	**Consortium Partners**
Editors	**Giuseppe Tommaso Costanzo, DTU CEE**
Date	**October 30, 2013**

Funding: Joint by partners and Danish Government (iPower platform has been granted support from SPIR - Strategic Platform for Innovation and Research).

DOCUMENT CONTROL

Members of the iPower Consortium

Balslev	BALSLEV
CITRIS	CITRIS
COWI	COWI
Danfoss	DANFOSS
Danish Energy Association	DE
Kolding School of Design	KSD
DEVELCO Products	DEVELCO
DONG Energy	DONG
DTU Centre for Electric Technology	DTU CET
DTU Informatics	DTU IMM
DTU Management Engineering	DTU MAN
Electronic Houskeeper	HOUSEKEEPER
ENFOR	ENFOR
Greentech Solutions	GREENTECH
Greenwave Reality ApS	GREENWAVE
Grundfos A/S	GRUNDFOS
IBM Denmark	IBM
University of Illinois	ILLINOIS
KPMG	KPMG
Lodam Electronics	LODAM
Lund University	LUND
National Consumer Research Centre	NATIONAL CONSUMER
NeoGrid Technologies ApS	NEOGRID
Nilan A/S	NILAN
Nordjysk Elhandel A/S	NEAS
QEES	QEES
Risø DTU	RISØ DTU
Saseco	SASECO
Danish Technological Institute	TI
University College Dublin	DUBLIN
Vestfrost Solutions	VESTFROST
Vestas	VESTAS
Zense Technology	ZENSE
Aalborg University	AAU

List of Contributors

Giuseppe Tommaso Costanzo, DTU CEE	WP1 participant

List of Reviewers

Søren Østergaard Jensen, DTI	WP1 leader
Oliver Dufour, GWR	WP1 participant
Henrik William Bindner, DTU CEE	WP4 participant
Jacopo Parvizi, DTU IMM	WP4 participant

Latest Version of this Document

Podio

Related Documentation

iPower Glossary
iPower Flexibility Interface - Information Model for Direct Control

Summary of Changes

Version 0.1 29/10/2012, Giuseppe T. Costanzo	Document created.
Version 0.2 16/01/2013, Giuseppe T. Costanzo	Document updated with building modeling.
Version 0.3 11/05/2013, Giuseppe T. Costanzo	Document updated with appliances modeling, first draft circulated.
Version 0.4 03/05/2013, Giuseppe T. Costanzo	Document updated with comments from Søren Jensen, Oliver Dufour, Henrik Bindner, Jacopo parvizi.
Version 1 30/10/2013, Giuseppe T. Costanzo	Document cleared by iPower consortium for public release.

Contents

1 INTRODUCTION

Abour Smart Grids. In many countries in the EU and in the United States, coil and nuclear plants provide the majority of energy production [2, 3], while peak absorption is matched by regulation plants and power exchange between grids. Throughout the last two decades, factors, such as increased global energy demand, speculation of fossil fuels, and global warming have generated a high interest in renewable energy sources. Nevertheless, energy sources, such as wind and solar power, have an intrinsic variability that can seriously affect the power grid stability if they account for a high percentage of the total generation. To face these challenges, the scientific community, as well as many industrial sectors, are taking steps to upgrade electrical network infrastructures and related technologies to ensure energy production and deliverance through the next century. The **Smart Grid** is a new paradigm for electric energy systems, which can intelligently integrate the actions of such actors as: generators, consumers and those that do both, in order to efficiently deliver sustainable, economic and secure electricity supplies [4]. Such scenario requires from consumers (and also producers) a certain **flexibility**, referred as the capability of a device or cluster of devices to change the power consumption or production in time and magnitude. This behavior can be granted by local controllers or supervisory controllers who are able to operate under the direct or indirect control paradigm [5]. Typical devices that offer flexibility are thermal and electrical storages, whose internal temperature or state of charge (SOC) is to be kept within specific comfort bounds. Alternatively, also PV plants can offer flexibility as soon as the controlling inverters are capable of controlling the power output.

About Demand-side Management. The World Business Council for Sustainable Development estimates that in most developed countries buildings account approximately for the 30-40 % of total energy consumption [6]. Energy consumption in a building can be related to such applications as space heating and building automation (including security systems and ICT infrastructures) or to human activities. It emerges that controlling loads with building automation systems can enhance the overall demand flexibility and enable a win-win situation, where customers adjust their consumption upon economic inducements and utilities avoid grid overloads by spreading the demand during the off-peak time [7]. Such technology is known as Demand-side Management, and buildings where the information infrastructure enables energy and operational savings through continuous data-driven analytics and remote control actions are here defined as **Smart Buildings**.

About iPower. Danish policy makers foresee that by the year 2025, half of the energy consumption in Denmark will be matched by renewable energy, most of which will be wind energy [8]. In order to develop intelligent control of power consumption and production at distribution level, the Danish Strategic Platform for Innovation and Research (SPIR) has granted the iPower consortium with 60 billion Danish Kroner, which consists in a collaboration of 32 partners including universities, research institutions and industrial companies seeking to release the growth and innovation potential in the Danish industry for development and production of smart grid tools. iPower will ensure the release of the growth and innovation potential in Danish industries for the development and production of intelligent decentralized power consumption and production control tools [9].

About this report. The mathematical description of physical systems and phenomena allows formalizing control problems, which diversity in complexity and applications is unified in the control theory. Therefore, validated models of energy consumption are necessary in the phases of design, test and benchmark of any control system. The first part of this report presents a modeling approach and a set of models for household loads, which are essential for the design and test of DSM technologies. The second part presents the implementation of such models in a simulation platform, showing how all the models can be connected and contribute to the simulation of the whole building consumption. The chosen platform for simulation is Matlab/Simulink.

2 MODELING BUILDING THERMAL CONSUMPTION

Most of the buildings exhibit a high thermal inertia, meaning that the heating system can be controlled with a certain degree of flexibility with respect of runtime and power consumption in order to keep the internal temperature between given comfort bounds. The flexibility of the heating system depends by such factors as: user preferences (the narrower is the comfort band, the smaller is the flexibility), building occupancy and ambient conditions such as: solar radiance, external temperature and wind speed and direction. This perspective motivates the development of models for building heat demand which, by means of resistive electric heating or heat pumps, can be related to the electric demand.

2.1 MODELS AS REPRESENTATION OF REALITY

"When dealing with scientific or technical problems, it is always possible to distinguish, more or less well, three moments: the first is the summarization of facts or phenomena under study and the formalization of the problem with equations; the second phase consists in the manipulation of equations in order to obtain the elements that are accessible in experimental trials; the third phase, finally, is the one in which the elements deducted from theory are compared with experimental results," cit. Ercole Bottani (1935).

Mathematical models allow to use standard techniques to deal with control problems of different nature and complexity, from physics, to electronics, to social science and biology. Therefore, thanks to mathematical modeling, each problem is first transformed from the real world to the mathematical world (modeling problem). The successive step consists in the design of the controller (synthesis problem), after which follows the realization of the controller, back in the real world. The conclusive procedure consists in the validation of the control system via simulation and experimental results (analysis problem).

In general, the complexity of the control system is directly related to the complexity of the controlled system, so that it is in general possible and convenient to use simplified models in the synthesis problem. However, in the analysis problem it is common practice to validate the controller with accurate models of the system under control before proceeding with the implementation of the controller. A recent achievement of control engineering is the HIL (hardware-in-the-loop) simulation, where most of the system (including the controller) is simulated, while some critical components are real and opportunely interfaced to the simulation environment via dedicated hardware and software.

In the context of building thermal management, the goals for control design are:

- keep the user comfort at adequate level;
- offer consumption flexibility to the Power System;

so that it emerges that building thermal models should relate the electric energy consumption for climate control to the evolution of the internal temperature. The influence of ambient conditions, whether they are measurable, and building occupancy should be also explicitly accounted in the model. Clearly it is worth to design models of adequate complexity in relation to the control goals, as trade off between performances and complexity.

In this paragraph two grey-box models of different complexity are presented for an office building. **Grey-box modeling** is a technique that not only provides a comprehensive physical and statistical description of the system, but also allows to define the model structure and parameters based on the prior knowledge of the system. Building physical characteristics such as: U-value, thermal capacity, windows area and surface exposed to sun can be directly accounted in the grey-box models. Therefore, it emerges that this class of models is convenient to developed intelligent climate control for DSM applications, which performances are assessed with respect the temperature evolution and the consumption flexibility.

2.2 GREY-BOX MODELING OF BUILDING THERMAL CONSUMPTION

This chapter presents two models for heat demand of Power FlexHouse, an office building consisting of 8 rooms connected to SYSLAB research facility. Power FlexHouse is equipped with 10 electric space heaters (one per room and two in rooms 7 and 8) and cooled by 5 air conditioners (in rooms 1, 2, 3, 4, 8). Tap water comes from a hot water storage tank and the space is illuminated by 24 fluorescent lamps. There is a small kitchen consisting of a fridge and a coffee machine. Heaters, air conditioners, water boiler and lamps are remotely controlled. The state of the building and appliances is read from various sensors and a software infrastructure offers interfaces to all devices and access to the house's state in Fig. 1.

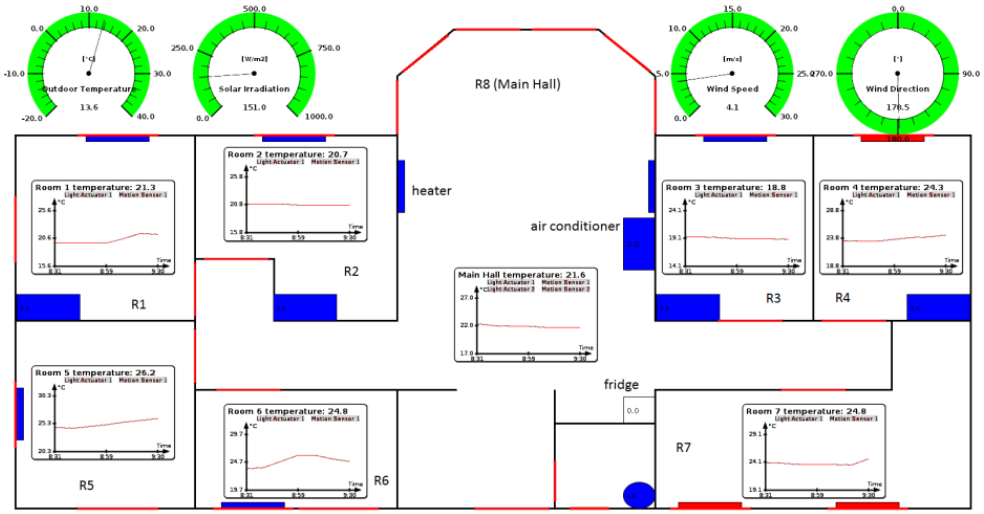

Figure 1: Power FlexHouse layout and state information panel.

Citing [1], the problem of identifying a suitable model is both finding a model that is in agreement with the physical reality and finding a model, which has a complexity that is in agreement with the level of information embedded in data, which means that the model should neither be under-fitted nor over-fitted.

The three studies [1], [10] and [11] present models for building heat dynamics based on the grey-box modeling via Stochastic Differential Equations (SDE). The heat exchange equations are derived thanks to the prior knowledge of the building structure and then parameters are identified on the basis of measured data. Being the system input the thermal power, the building thermal dynamics are excited via Pseudo-binary random sequence (PRBS) that controls the heaters. The grey-box approach is of the most interest since it allows to obtain models which parameters are lumped and, having physical meaning, can be related to specific characteristics of the building (e.g., size, amount of windows, thermal inertia, U-value). **Lumped parameter models** simplify the description of the behavior of spatially distributed physical systems into a topology consisting of discrete entities that approximate the behavior of the distributed system under certain assumptions.

The first approach, on which are based models in [1] and [10], is based on a one room-equivalent representation of the building and is useful to estimate the overall building heat demand and simulate the rooms average temperature assuming the heat power is equally dispatched among the rooms. This model offer the relevant advantage of being simple and of low order. Conversely, the second model, published in [11] and reported in Section 2.2.2, accounts for each single room dynamics and for cross-room coupling effects, being based on a multi-room representation of the building. This second model is of higher order and allows to simulate and control the temperature in each room; such model is of interest for the

analysis phase.

Model parameters are estimated using CTSM, which provides a tool for semi-physical modeling and identification of dynamic systems based on stochastic differential equations [12]. CTSM estimates unknown parameters of the model from data via maximum likelihood (ML) method and a maximum a posteriori (MAP) method [13]. Both methods allow several independent data sets to be used and are both statistics-based, which means that once the parameters have been estimated, statistical methods can be applied to investigate the quality of the model [14].

2.2.1 SINGLE-ROOM MODEL

This section presents a model of the Power FlexHouse which is formulated as one large room exchanging heat with the external environment [10]. This crude approximation is convenient to catch the dominant heat dynamics of the building, which allows estimating and predicting its overall heat demand. With such approach, the space heating and cooling is modeled as a single appliance, so that it is not possible to control the temperature in rooms individually but control the average temperature among all the rooms.

Three states are used to describe the building heat dynamics: the first state is the indoor air temperature, T_i, the second state is the temperature of the building envelope, T_{om}, and the third state is the temperature of the inner walls layers and floor, T_{im}. The inner part of FlexHouse receives energy from solar irradiation through the windows. Figure 2 presents the thermal circuit for the proposed model (right) and a representation of heat flows (left):

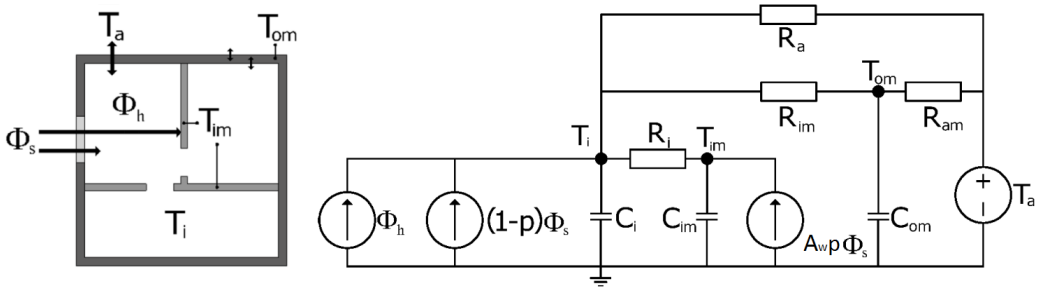

Figure 2: Thermal circuit for single room model of Power FlexHouse.

Assuming that the energy flow due to solar radiation is not absorbed by the outer walls layer, the energy is distributed between the inner walls layer and the indoor air. If p is the part of the solar radiation which directly affects the inner walls layer temperature, T_{im}, the energy flow due to solar radiation is given by:

$$\begin{aligned} \dot{Q}_{im} &= A_w p \Phi_s \\ \dot{Q}_i &= A_w (1-p) \Phi_s \end{aligned} \quad . \tag{1}$$

Therefore the differential equation for the inner wall layer temperature is:

$$C_{im} \frac{dT_{im}}{dt} = hA(T_i - T_{im}) + \dot{Q}_{im} = \frac{1}{R_i}(T_i - T_{im}) + A_w p \Phi_s + \hat{R}_{11,1} d\omega_1 \ , \tag{2}$$

where C_{im} is the total heat capacity of the inner walls, Φ_s is the solar radiation, R_i is the total thermal resistance between the inner walls and the indoor air, A_w is the total windows surface and $\hat{R}_{11,1}$ is the diffusion term, which gives information

for pinpointing model deficiencies [15]; finally, ω_1 is a Markov process representing the uncertainty in the model. The house envelope exchanges heat by convection to both the inside and the outside of the building:

$$C_{om}\frac{dT_{om}}{dt} = \frac{1}{R_{im}}(T_i - T_{om}) + \frac{1}{R_{am}}(T_a - T_{om}) + \hat{R}_{22,1}d\omega_2 \ , \tag{3}$$

where T_{om} is the outer walls layer temperature, C_{om} is the thermal capacity of the outer walls, R_{im} and R_{am} are the thermal resistances from outer wall layer towards the indoor and outdoor and $\hat{R}_{22,1}$ is the diffusion term.

The indoor air exchanges heat to the external ambient by ventilation and conduction through the windows. Moreover, there is a heat exchange by convection between the air and both inner and outer walls. Finally, the indoor air also receives thermal energy from solar radiation and the electrical space heaters, accounted in the terms Φ_s and Φ_h. Therefore the equation for the heat balance of the indoor air follows:

$$C_i\frac{dT_i}{dt} = \frac{1}{R_a}(T_a - T_i) + \frac{1}{R_i}(T_{im} - T_i) + \frac{1}{R_{im}}(T_{om} - T_i) + A_w(1-p)\Phi_s + \Phi_h + \hat{R}_{33,1}d\omega_3 \tag{4}$$

where C_i is the total heat capacity of the indoor air, R_a is the total resistance against heat flow to the outside, through windows and due to ventilation, and is the energy input from the electrical heaters. Also this equation presents the diffusion term $\hat{R}_{33,1}$. Finally, the measured temperature, T_r, is given by:

$$T_r = T_i + \hat{R}_2 d\omega_4 \tag{5}$$

The model parameters are estimated with CTSM [12], and the parameters of Eq. 2, 3, 4 are presented in Table 1:

Parameter	Exp. Value	St. Dev.
R_i	$4.68E+01\ ^\circ C/kW$	$1.34E-01$
C_i	$8.12E+00\ kWh/^\circ C$	$2.94E-01$
R_{im}	$1.81E+00\ ^\circ C/kW$	$0.15E+00$
R_a	$8.02E+00\ ^\circ C/kW$	$0.50E+00$
C_{im}	$5.53E-03\ kWh/^\circ C$	$6.11E-04$
C_{om}	$2.93E+02\ kWh/^\circ C$	$7.68E+00$
R_{am}	$8.46E-02\ ^\circ C/kW$	$2.94E-02$
A	$2.02E+01\ m^2$	$1.49E+00$
p	1	0
$log(\hat{R}_{11,1})$	$-2.754E+00\ ^\circ C^2$	$2.99E-01$
$log(\hat{R}_{22,1})$	$6.38E+01\ ^\circ C^2$	$5.86E-02$
$log(\hat{R}_{33,1})$	$-9.43E-01\ ^\circ C^2$	$3.12E-01$
$log(\hat{R}_2)$	$-7.07E+00\ ^\circ C^2$	$7.55E-02$

(a) Parameters in case of fixed p=1.

Parameter	Exp. Value	St. Dev.
R_i	$4.80E+01\ ^\circ C/kW$	$1.02E-01$
C_i	$8.12E+00\ kWh/^\circ C$	$4.71E-01$
R_{im}	$1.81E+00\ ^\circ C/kW$	$2.43E-01$
R_a	$8.03E+00\ ^\circ C/kW$	$1.65E+00$
C_{im}	$5.40E-03\ kWh/^\circ C$	$6.11E-04$
C_{om}	$2.95E+02\ kWh/^\circ C$	$8.03E+00$
R_{am}	$8.35E-02\ ^\circ C/kW$	$3.32E-02$
A_w	$2.02E+01\ m^2$	$1.49E+00$
p	$9.95E-01$	$1.33E-02$
$log(\hat{R}_{11,1})$	$-2.75E+00\ ^\circ C^2$	$3.48E-01$
$log(\hat{R}_{22,1})$	$6.39E+00\ ^\circ C^2$	$6.9E-02$
$log(\hat{R}_{33,1})$	$-0.94E+00\ ^\circ C^2$	$0.31E+00$
$log(\hat{R}_2)$	$-7.07E+00\ ^\circ C^2$	$8.48E-02$

(b) Parameters in case of identified p.

Table 1: ingle-room model parameters.

The continuous-time model in Eq. 2, 3, 4 is then discretized with a step of 5 min for simulation and control. Figure 3 presents the model fit: in the upper chart, measured (red) and one-step prediction of (blue) internal temperature are compared, whereas the lower chart shows the model residuals.

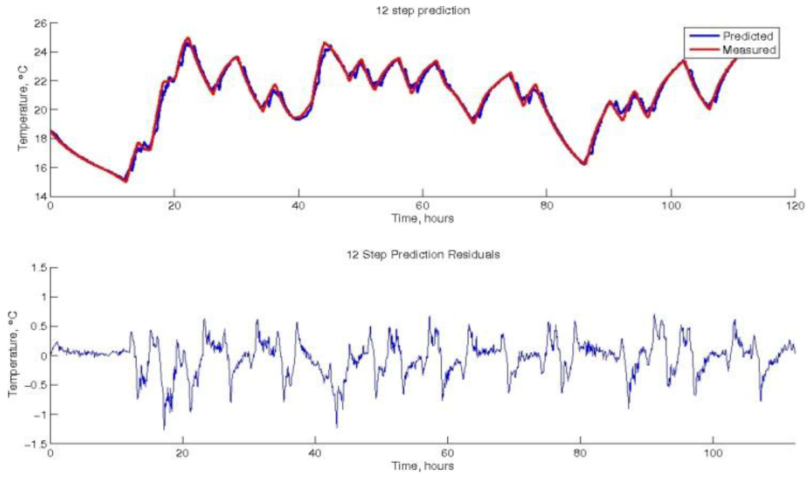

Figure 3: Measured vs. predicted temperature and residuals.

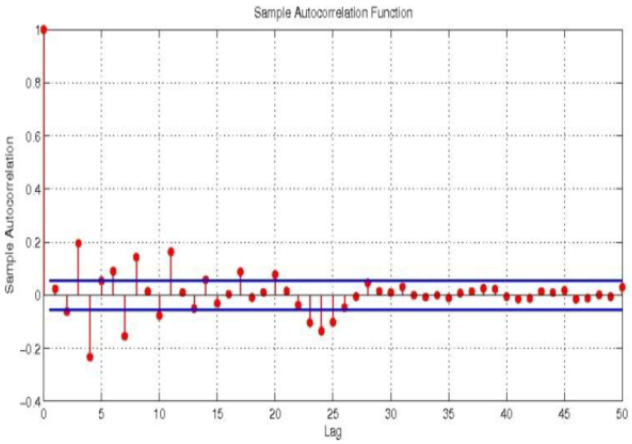

(a) Autocorrelation function (lag of 5 minutes).

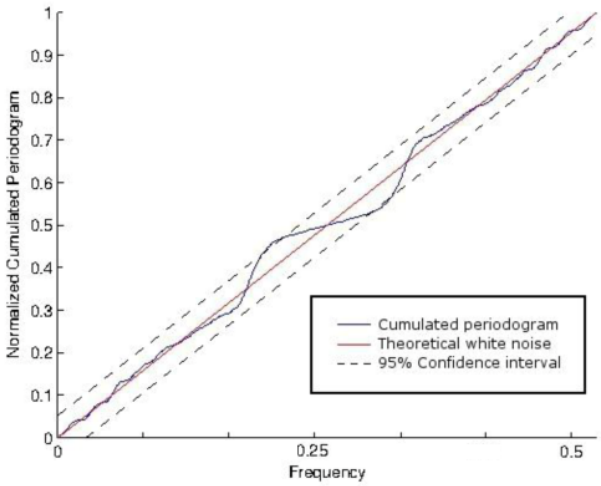

(b) Cumulative periodogram (normalized to the Nyquist frequency).

Figure 4: Model validation: one step prediction

Figure 4 presents the autocorrelation function (ACF) in the left chart and the cumulative periodogram in the right chart of the model residuals. The autocorrelation function shows whether the prediction errors are correlated in time. A high correlation expresses model inaccuracies, as the error is systematic and therefore it can be compensated. From the ACF we notice that the model is not highly accurate in catching some of low frequency dynamics, that is depicted by the fact that the model residuals are somehow correlated for low values of lags. Note that one lag is one time sample (5 minutes). For more information and a mathematical insight on the techniques used for model validation, the interested reader can refer to [16].

A similar approach for single-room models is presented in [1], where models of different complexity are presented and compared. Model selection is done via forward model selection evaluating different performance criteria, such as the Akaike Information Criterion (AIC), Maximum Description Length (MDL) or Final Prediction Error (FPE). Models of increasing order are tested and their complexity is traded-off with prediction performances.

About the cumulative periodogram (taken from [17]). *"A basic idea in mathematics and statistics is to take a complicated object (such as a time series) and break it up into the sum of simple objects that can be studied separately, see which ones can be thrown away as being unimportant, and then adding what's left back together again to obtain an approximation to the original object. The periodogram of a time series is the result of such a procedure. Given a time series data set of length n (assumed to be even for now for convenience), it is possible to find cosines and sines of periods* $n; n/2; ...; n/(n/2) = 24$ *that when added together [...] give the data set back again. The basic idea is that sinusoids of low frequency (or equivalently long period) are smooth in appearance whereas those of high frequency (or short period) are very wiggly. Thus if a time series appears to be very smooth (wiggly), then the values of the periodogram for low (high) frequencies will be large relative to its other values and we will say that the data set has an excess of low (high) frequency. For a purely random series, all of the sinusoids should be of equal importance and thus the periodogram will vary randomly around a constant [...]. A useful tool for describing the overall behavior of the periodogram (and thus the data set) is the* ***cumulative periodogram****,* F*. Note that for a purely random series,* F *should follow along a line from* $(0; 0)$ *to* $(0 : 5; 1)$*. For a series having excess of low (high) frequency,* F *will start out above (below) that* $y = 2x$ *line, while there will be a jump in* F *at any frequency where the time series has a peak."*

2.2.2 MULTI-ROOM MODEL

This section presents a multi-room model for the Power FlexHouse [11]. The aim of this model is to describe the individual rooms' heat dynamics, including the influence of the heaters, the solar radiation and the outside temperature. Disturbances caused by wind speeds are modeled as unknown noise.

Each room is represented as an element which is exchanging heat, not only with the outside environment, but also with the rooms that surround it. This approach creates cross-correlation terms in the model, which describe the behavior of the room heat dynamics depending on the adjoining rooms. Figure 5 presents the thermal circuit of room one, from which it is possible to depict the interaction with the adjacent rooms, two and five.

The innovations brought by the multi-room model are:

- cross-correlation terms between rooms, which provide a more precise model of the building;
- quasi-diagonal system, which allows to use the same identification approach used in [1] to identify full models for every single room.

Model inputs are:

- solar irradiance;

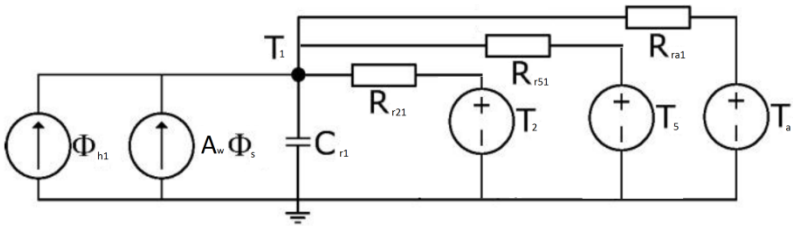

Figure 5: Thermal circuit for Room 1.

- outside temperature;
- thermal power generated by the heaters.

Following the grey-box physical modelling, multi-room model equations are presented below (T_{r0} represents the internal temperature of the main room):

$$
\begin{aligned}
C_{r0}\frac{dT_{r0}}{dt} &= \frac{1}{R_{ra0}}(T_a - T_{r0}) + \frac{1}{R_{r20}}(T_{r2} - T_{r0}) + \frac{1}{R_{r30}}(T_{r3} - T_{r0}) + \frac{1}{R_{r60}}(T_{r6} - T_{r0}) + \frac{1}{R_{r70}}(T_{r7} - T_{r0}) + A_{w0}\Phi_s + \Phi_{h0} + \sigma_{r0}\frac{dW}{dt} \\
C_{r1}\frac{dT_{r1}}{dt} &= \frac{1}{R_{ra1}}(T_a - T_{r1}) + \frac{1}{R_{r21}}(T_{r2} - T_{r1}) + \frac{1}{R_{r51}}(T_{r5} - T_{r1}) + A_{w1}\Phi_s + \Phi_{h1} + \sigma_{r1}\frac{dW}{dt} \\
C_{r2}\frac{dT_{r2}}{dt} &= \frac{1}{R_{ra2}}(T_a - T_{r2}) + \frac{1}{R_{r20}}(T_{r0} - T_{r2}) + \frac{1}{R_{r21}}(T_{r1} - T_{r2}) + A_{w2}\Phi_s + \Phi_{h2} + \sigma_{r2}\frac{dW}{dt} \\
C_{r3}\frac{dT_{r3}}{dt} &= \frac{1}{R_{ra3}}(T_a - T_{r3}) + \frac{1}{R_{r30}}(T_{r0} - T_{r3}) + \frac{1}{R_{r34}}(T_{r4} - T_{r3}) + A_{w3}\Phi_s + \Phi_{h3} + \sigma_{r3}\frac{dW}{dt} \\
C_{r4}\frac{dT_{r4}}{dt} &= \frac{1}{R_{ra4}}(T_a - T_{r4}) + \frac{1}{R_{r34}}(T_{r3} - T_{r4}) + \frac{1}{R_{r47}}(T_{r7} - T_{r4}) + A_{w4}\Phi_s + \Phi_{h4} + \sigma_{r4}\frac{dW}{dt} \\
C_{r5}\frac{dT_{r5}}{dt} &= \frac{1}{R_{ra5}}(T_a - T_{r5}) + \frac{1}{R_{r51}}(T_{r1} - T_{r5}) + \frac{1}{R_{r65}}(T_{r6} - T_{r5}) + A_{w5}\Phi_s + \Phi_{h5} + \sigma_{r5}\frac{dW}{dt} \\
C_{r6}\frac{dT_{r6}}{dt} &= \frac{1}{R_{ra6}}(T_a - T_{r6}) + \frac{1}{R_{r65}}(T_{r5} - T_{r6}) + \frac{1}{R_{r60}}(T_{r0} - T_{r6}) + A_{w6}\Phi_s + \Phi_{h6} + \sigma_{r6}\frac{dW}{dt} \\
C_{r7}\frac{dT_{r7}}{dt} &= \frac{1}{R_{ra7}}(T_a - T_{r7}) + \frac{1}{R_{r70}}(T_{r0} - T_{r7}) + \frac{1}{R_{r47}}(T_{r4} - T_{r7}) + A_{w7}\Phi_s + \Phi_{h7} + \sigma_{r7}\frac{dW}{dt}
\end{aligned}
\tag{6}
$$

The parameters of the continuous time model in Eq. 6 are identified via CTSM and presented in the Table 2. Note that

Figure 6 presents the model fit for each room, where the red line represents the predicted temperature and the blue line the measured temperature. The ACF of the model residuals are presented in Fig. 7.

Further details on this model are available upon request to the authors of [11].

2.3 OTHER MODELING APPROACHES (FROM [1]).

"[18] gives an overview of techniques for steady state and for dynamic analysis of energy use in a building, the latter implicate modeling of the heat dynamics of the building. Such dynamic models can be realized with a set of differential equations, as carried out by Sonderegger [19] and [20]. Parameter estimation in dynamical models is known as system identification and a survey of different approaches for buildings is found in [21]." A model of Power Flexhouse that accounts

Parameter	Exp. Value	Std.
R_{a1}	5.13E+01 $°C/kW$	1.19E+00
C_{r1}	1.97E+03 $kWh/°C$	3.62E-03
R_{21}	5.02E+01 $°C/kW$	6.14E+00
R_{51}	1.97E+02 $°C/kW$	2.18E+01
A_{w1}	4.29E-01 m^2	3.15E-02
σ_{r1}	-2.14E-01 $°C^2$	6.00E-03
R_{a2}	6.20E+05 $°C/kW$	5.80E+00
C_{r2}	4.98E-01 $kWh/°C$	2.56E-02
R_{20}	3.40E+01 $°C/kW$	1.11E+01
A_{w2}	6.97E-01 m^2	8.97E-02
σ_{r2}	-4.96E-01 $°C^2$	2.69E-02
R_{a3}	6.58E+01 $°C/kW$	5.33E+00
C_{r3}	4.52E-01 $kWh/°C$	3.19E-02
R_{30}	3.35E+01 $°C/kW$	9.84E+00
R_{34}	1.16E+02 $°C/kW$	1.29E+02
A_{w3}	6.21E-01 m^2	9.05E-02
σ_{r3}	-4.87E-01 $°C^2$	3.57E-02
R_{a4}	4.75E+01 $°C/kW$	4.52E+00
C_{r4}	6.77E-01 $kWh/°C$	6.91E-02
R_{a4}	4.75E+01 $°C/kW$	4.52E+00
R_{47}	1.99E+02 $°C/kW$	8.23E+00
A_{w4}	1.14E+00 m^2	1.58E-01
σ_{r4}	-7.42E-01 $°C^2$	7.67E-02

(a) Parameters: rooms 1-4.

Parameter	Exp. Value	Std.
R_{a5}	6,32E+01 $°C/kW$	3,69E+00
C_{r5}	3,93E-01 $kWh/°C$	2,33E-02
R_{65}	4,98E+01 $°C/kW$	8,31E+00
A_{w5}	8.37E-01m^2	7.46E-02
σ_{r5}	-4.36E-01 $°C^2$	2.74E-02
R_{a6}	6,59E+01 $°C/kW$	1,65E+00
C_{r6}	1,62E-01 $kWh/°C$	3,56E-03
R_{60}	5,43E+01 $°C/kW$	1,08E+01
A_{w6}	9.15E-02 m^2	2.64E-02
σ_{r6}	-1.74E-01 $°C^2$	5.26E-03
R_{a7}	5,36E+01 $°C/kW$	3,65E+00
C_{r7}	3,31E-01 $kWh/°C$	1,66E-02
R_{70}	8,37E+01 $°C/kW$	3,51E+01
A_{w7}	2.89E-01 m^2	4.76E-02
σ_{r7}	-4.22E-01 $°C^2$	2.28E-02
R_{a0}	2,31E+01 $°C/kW$	1,29E+00
C_{r0}	9,17E-01 $kWh/°C$	4,37E-02
A_{w0}	2.57E+00 m^2	1.64E-01
σ_{r0}	-1.18E+00 $°C^2$	5.94E-02

(b) Parameters: rooms 5-7, 0.

Table 2: multi-room model parameters. **Note that the parameters R presented here need to be multiplied by 300, which is the sampling time (in seconds) of experimental data, before being used in the continuous-time model 6**

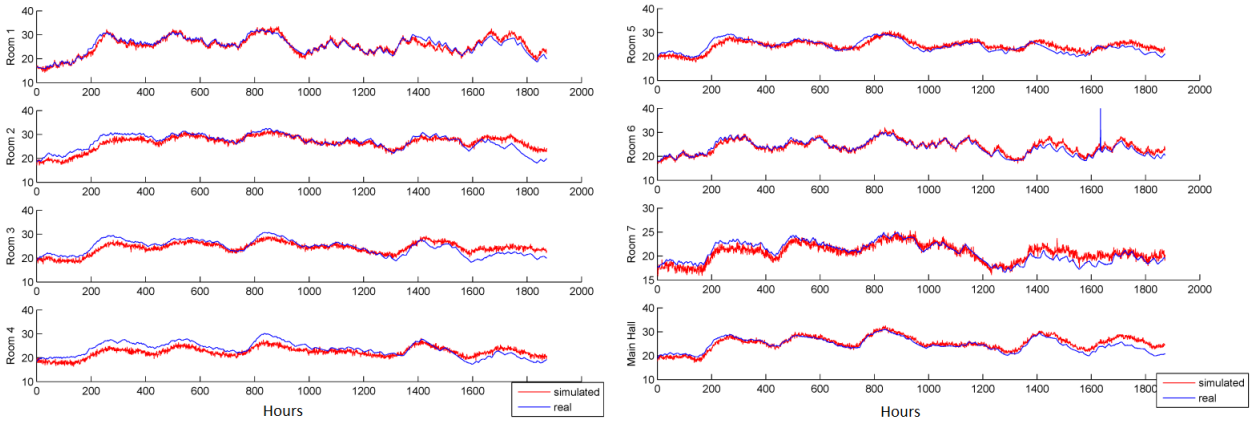

Figure 6: multi-room model residuals.

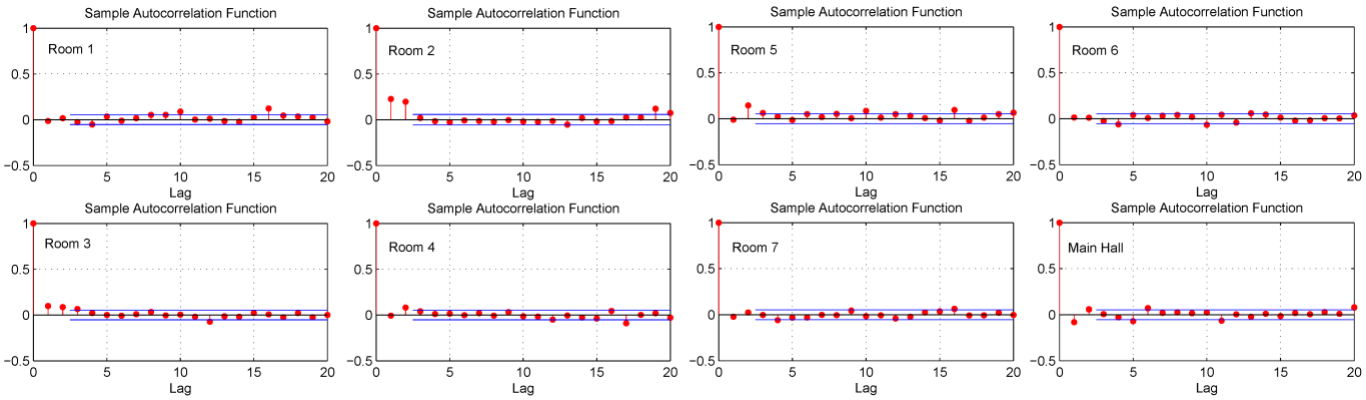

Figure 7: multi-room model residuals ACF per each room.

for non-linear effects of wind and air infiltration is proposed in [22], where the wind effect is modeled via non-linear U-value therm in the SDE model.

2.4 Concluding remarks

Modeling the building heat dynamics is a process that is far from being trivial and, in the case of grey-box approach, it requires a prior knowledge of the building structure [14]. However, when identifying models' parameters, it is necessary to operate simplifications and reduce model dimension in order to ease the identification and the control design processes.

Although it is possible to obtain different type of models for heat building demand, e.g. regression models relating the heat demand with the external temperature, the models described in this section relate the evolution of internal temperature to the heating power and the external conditions (air temperature and solar irradiation). This type of information is needed from the models in order to design control strategies for demand response since users' comfort is a major issue in such context. These models are can be used to implement model predictive controllers (MPC) for space heating and cooling, which allow optimizing the consumption with respect the energy price (in a D/R environment) and also the local production (where it is available).

3 Modeling household refrigerator consumption

This chapter presents the modeling of a vapor-compression refrigeration system for residential applications via grey-box approach. Household refrigerator modeling and performance assessment has been previously addressed with such approaches as dynamic simulation [23], steady state simulation [24], or CFD models [25]. The lumped-parameter model presented in this chapter provides a simple, ready-to-use tool for simulation and control of household refrigerators.

The interest is in controlling the refrigerator as flexible consumption unit, which operation can be shifted within temperature and operational constraints. In case the refrigerator is not intended to be used as smart load, validated models are useful for predicting unit consumption. This information is useful for the management of other flexible units, such as heat pumps for space heating, in order to smooth the load factor during peak hours. The goal is to obtain a model that relates the power consumed by the compressor (input) and the external temperature (disturbance) to the temperature of the refrigeration chamber (controlled variable) [26].

Figure 8 shows a simplified representation of a common refrigeration system for household applications, where the thermal exchange between the external ambient and the refrigeration chamber, the refrigeration chamber and the evaporator, the condenser and the ambient are enlightened.

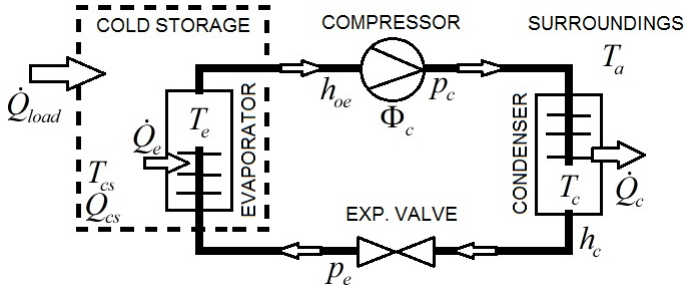

Figure 8: simplified single stage vapor compression refrigeration system.

Assuming that in most of the operational time the temperature gap between the refrigeration chamber and the external ambient slightly oscillates around a constant value, it is plausible to assume constant coefficient of performance (COP):

$$COP = \frac{thermal\ power}{electrical\ power} = \frac{\dot{Q}_e}{\Phi_c} \tag{7}$$

This system is described by the following equations:

$$\begin{aligned} dQ_{cs} &= m_{cs} c_{cs} dT_{cs} \\ \dot{Q}_{load} &= UA_{cs} (T_a - T_{cs}) \\ \dot{Q}_e &= \dot{m}_r [h_{oe}(p_e) - h_{oc}(p_c)] \approx COP \cdot \Phi_c \\ \dot{m}_r &= N_c \alpha \rho_r (p_e) \end{aligned} \quad , \tag{8}$$

where m_{cs} is the cold storage mass and c_{cs} is its specific heat. UA_{cs} is the overall heat transfer coefficient from refrigeration chamber to the ambient. $\dot{m}_r$ is the refrigerant mass flow; h_{oe} and h_{oc} are the refrigerant evaporation and condensation enthalpies, while p_{oe} and p_{oc} are the respective pressures. N_c is the compressor revolution speed, α is a scaling coefficient that depends on the mechanical configuration of the compressor and ρ_r is the refrigerant viscosity.

Reporting the study presented in [26], a good compromise between model complexity and accuracy is provided by the two-states lumped-model depicted in Fig. 9b. In this model a state is assigned to the evaporator and the refrigeration chamber. Figure 9a shows the positioning of the temperature sensors in the experimental setup.

The readings from sensors T1 and T2 are averaged to obtain the refrigeration chamber temperature, while the readings from T3 and T4 are averaged to obtain the ambient temperature. Follow the model equations:

$$\begin{aligned} dT_i &= \left[\tfrac{1}{C_i R_{ia}} (T_a - T_i) + \tfrac{1}{C_i R_{ei}} (T_e - T_i) \right] dt + \sigma_1 dw_1 \\ dT_e &= \left[\tfrac{1}{C_e R_{ei}} (T_i - T_e) - \tfrac{1}{C_i} \cdot COP \cdot \Phi_c \right] dt + \sigma_2 dw_2 \\ y &= T_i + e_1 dv_1, \qquad w_1 \perp w_2 \perp v_1 \sim N(0,1) \end{aligned} \quad , \tag{9}$$

where T_i and T_e are the temperatures of refrigeration chamber (internal temperature) and evaporator; T_a is the ambient temperature. Model parameters are identified for empty refrigerator by using CTSM-R; the system is excited by operating the compressor on the basis of a PRBS. Note that model identification is carried out for empty refrigerator and a study

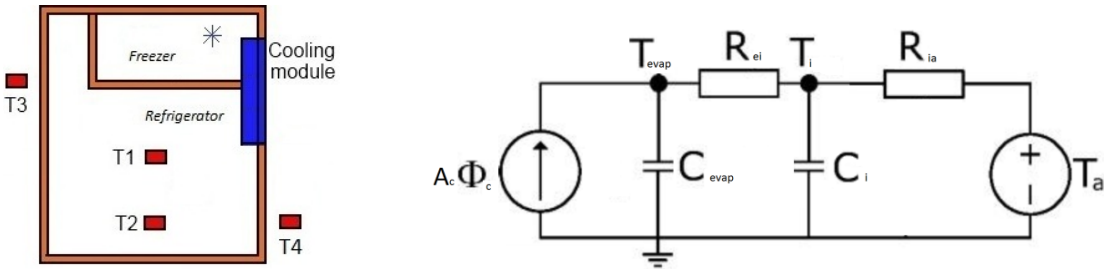

(a) Sensors setup.

(b) Thermal equivalent circuit.

Figure 9: refrigerator modeling.

Parameter	Exp. Value	Std.
R_{ia}	1.10E+00 $°C/kW$	2.11E+00
R_{ei}	5.19E-01 $°C/kW$	1.65E-01
C_i	8.97E+03 $kWh/°C$	1.77E+04
C_e	2.18E+02 $kWh/°C$	5.63E+01
COP	6.77E-01	1.30E+00
$log(\sigma_1)$	-1.28E+01 $°C^2$	6.93E-01
$log(\sigma_2)$	-1.97E+01 $°C^2$	1.69E+00
$log(e_1)$	-1.13E+01 $°C^2$	8.63E-02

Table 3: refrigerator model parameters.

that will assess foodstuff thermal inertia and its effects on flexibility is foreseen as next development. Follow the identified parameters of the continuous-time model in Eq. 9:

Figure 10a presents the input data to the estimation process: room temperature, refrigeration chamber temperature and power consumed by the compressor. On the right, Fig. 10b presents the model residuals, the power consumed by the compressor; in the third chart a comparison between measured and predicted temperature of the refrigeration chamber is presented, where the black curve represents the measured data and the red curve the model output (one-step prediction).

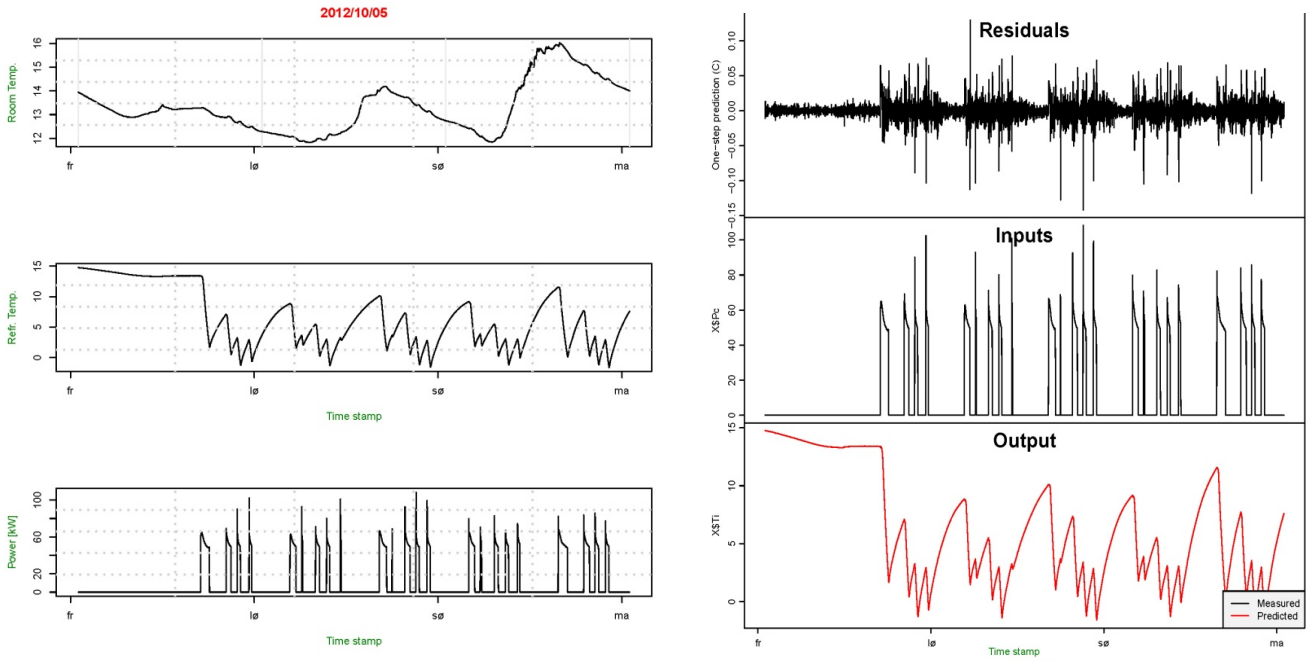

(a) Estimation data set (from top): T_a, T_i and Φ_c.

(b) Model residuals.

Figure 10: refrigerator model performances.

Figure 11 presents the ACF of model residuals, the residuals spectrum and the cumulative periodogram. The ACF shows small correlation at low frequency dynamics, which could be determined by approximations introduced by the lumped parameters representation of the evaporator dynamics and approximations in general in the refrigeration cycle modeling.

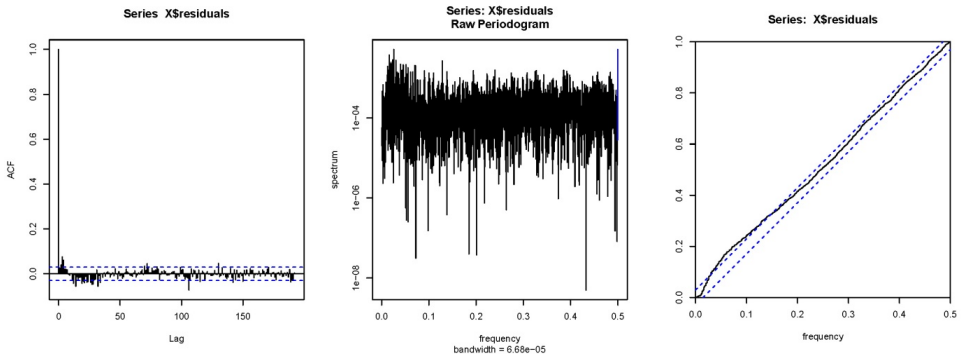

Figure 11: analysis of refrigerator model residuals: residuals ACF, periodogram and cumulated periodogram.

4 MODELING A GENERIC APPLIANCE

Any generic appliance whose operation is directly managed by a local control system and where power consumption is weakly influenced by external ambient conditions, as for example TV set or tumble dryer, can be easily represented by its power consumption profile associated to a specific operation mode. In any case the appliance operation is determined by the interaction with users, who operate the device in time and choose the operation mode. The use of finite state machines is particularly convenient for modeling such devices. Figure 12 presents a generic finite state machine (FSM) for appliances modeling.

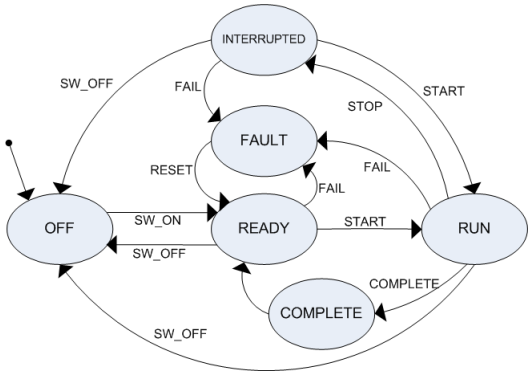

Figure 12: FSM representation of generic appliance.

Appliance status can be:

- Off: appliance not enabled;
- Ready: enable asserted, appliance ready to start;
- Run: enable asserted and start command received, appliance consuming energy;
- Interrupted: enable asserted and stop command received, appliance not consuming energy;
- Complete: task completed and transit to “Ready" for being turned off or possible re-invoke;

- Fault: fault detected in the appliance.

To every state of the FSM model is associated a power consumption profile (active/reactive) and other process parameters, such as elapsed time, possibility for process preemption, remaining time, etc. This approach allows to couple physical models with statistical models for usage patterns, as for example time of use, type of usage, etc. To implement models of this type it is required to map the device operation states and measure the power consumption associated to each one. The operating programs, such as different washing cycles of a dishwasher, are mapped in terms of power consumption profile. At simulation time the FSM model associates to each state a power consumption profile. Such model can be implemented with the interface presented in Fig. **??** in order to fit in the architecture proposed in [27].

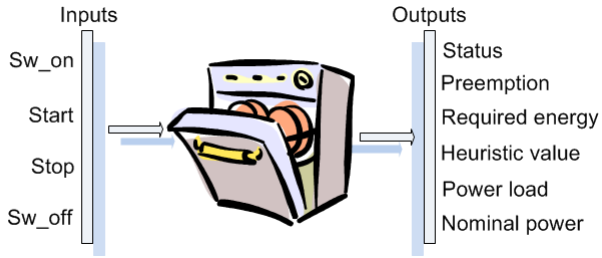

Figure 13: FSM information interface.

The trigger inputs: Sw_on and Sw_off are coming from the user interface and correspond to the user action of switching on or off the power supply. The Run and Stop triggers are coming either from the user or from the DSM system, depending whether it is intended to use the device for flexible consumption or not. The next section presents the consumption patterns for two appliances of common use in a kitchen: dishwasher and microwave oven.

4.1 DISHWASHER

Figure 14 presents a typical consumption pattern for the analyzed dishwasher in full load conditions. The blue line presents the active power consumed in kW and the green line the power factor (from which it is possible to compute the reactive power consumed):

The cycle depicted in Fig. 14 has the following main characteristics:

- Total apparent energy: 1.103 kVAh
- Total active energy: 1.079 kWh
- Cycle length (hh:mm:ss): 01:20:00

By analyzing the pattern is it possible to recognize the water heating cycle by noting that it is characterized by a high active power consumption, a unitary power factor (due to the resistive heating element), and it comes at the beginning of the cycle. Same characteristics are found in the drying cycle, except that it comes after the washing cycle that is characterized by low power consumption and a low power factor due to the power electronics controlling the pumps motors. Figure 14 and 15 present the consumption pattern for the same dishwasher, but respectively for three-fourth and half loading conditions. No relevant difference in terms of total energy consumed and cycle length is depicted. However, it might be possible that more sophisticated devices have different operation programs for different load conditions.

The cycle depicted in Fig. 15 has the following main characteristics:

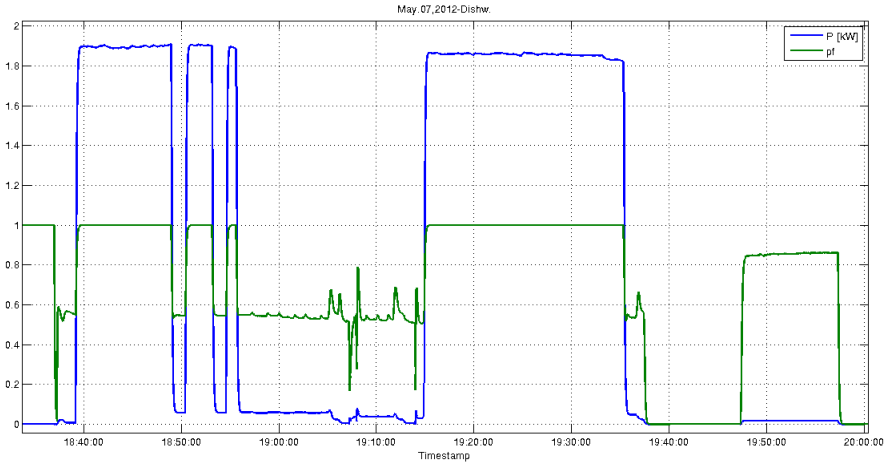

Figure 14: dishwasher consumption pattern (full load).

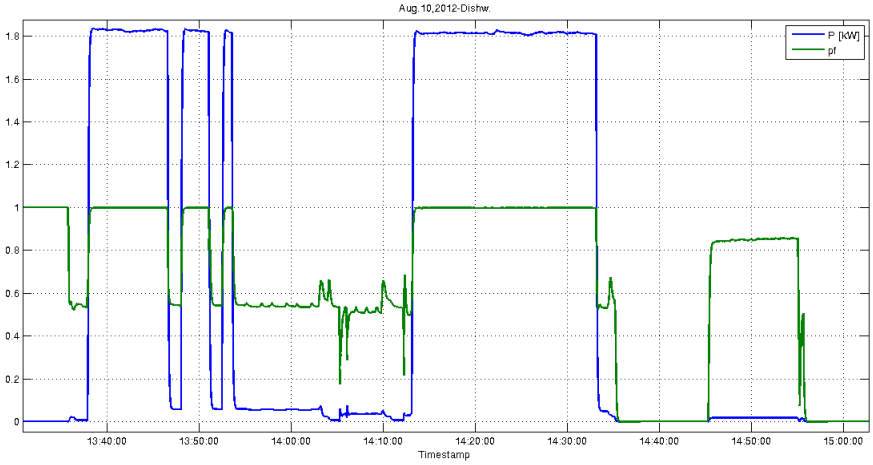

Figure 15: dishwasher consumption pattern (3/4 load).

- Total apparent energy: 1.296 kVAh
- Total active energy: 1.046 kWh
- Cycle length (hh:mm:ss): 01:20:32

The cycle depicted in Fig. 16 has the following main characteristics:

- Total apparent energy: 1.206 kVAh
- Total active energy: 1.059 kWh

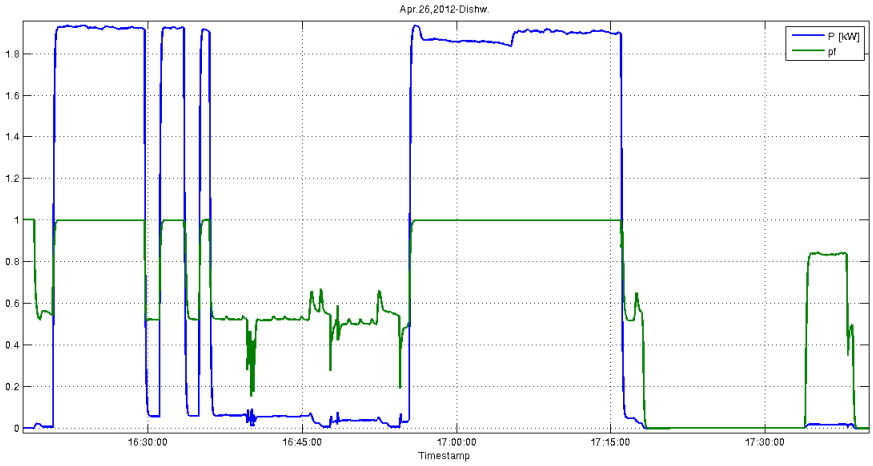

Figure 16: dishwasher consumption pattern (1/2 load).

- Cycle length (hh:mm:ss): 01:20:07

It is plausible to assume that the dishwasher here modeled can be simulated regardless the loading conditions with one standard consumption pattern. However, to show the framework capabilities, the block setup interface allows choosing among different measured patterns.

4.2 MICROWAVE OVEN

This section presents the measurement of microwave oven consumption for different operation modes. Figure 17 shows the âĂIJQuick reheatâĂİ cycle for different run times: one, two and three minutes.

This pattern record shows the following operation cycles (time, cycle type, required energy):

1.) 12:36 - Quick (3 min), 91.09 Wh
2.) 13:03 - Quick (3 min), 89.41 Wh
3.) 13:09 - 2 times Quick (1 min), 2*13.6 Wh
4.) 13:12 - Quick (2 min), 28.1 Wh
5.) 13:15 - Quick (3 min), 91.27 Wh

By inspecting the consumption pattern for this appliance, it is possible to depict that the relationship between the amount of energy consumed and the cycle length is nonlinear. In addition, equal of cycles with equal operation time do not require the same energy consumption. This characteristic could be related to the amount of food to be heated. Further investigations are intended to clarify this point and will constitute an extension of this report.

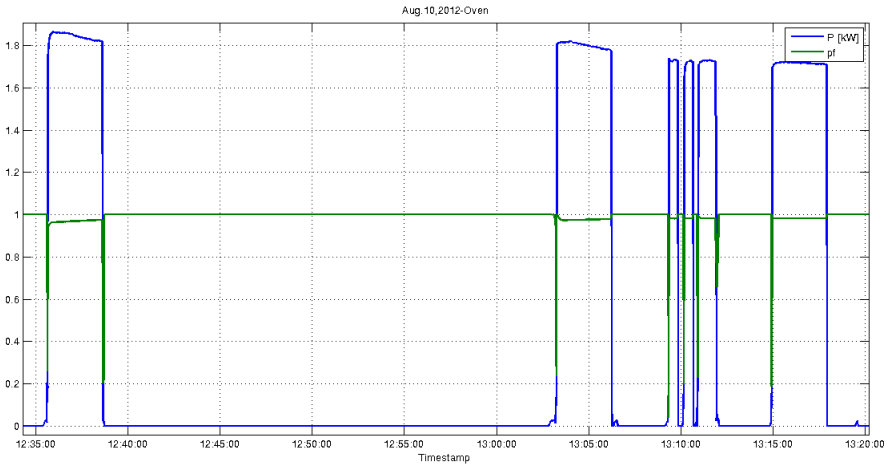

Figure 17: microwave oven consumption pattern.

5 SIMULINK IMPLEMENTATION

This chapter presents the implementation of the appliances models in Simulink, which is chosen together with Matlab for the possibility of being interfaced with other softwares power systems simulation and for offering extensive tools for control design and system analysis.

Appliances models are encapsulated in blocks which can be organized in libraries. Thereafter, it is possible to create a model for aggregated building consumption by creating a new Simulink model and adding the blocks corresponding to the desired appliances. In this way the simulation setup is modular, and can be easily modified to accommodate more and different devices. Each block implements a specific model, which can be modified to accommodate different simulation needs.

To create a new appliance model it suffices to store the power consumption profile in a .csv file and load it in the generic appliance block. In this way the generic appliance model is set to represent a specific device. With respect to thermal processes, such as water heaters, space heating and cooling systems, it is necessary to implement directly the differential equations. Figure 17 presents the configuration menu of the generic appliance block, which is accessed by right-clicking on the block and by choosing "Edit mask". In the Initialization pane it is possible to load the P-Q time series, which has to be resampled according to the simulation time sampling. The functions for profile loading and resampling are provided and need to be placed in the model working path.

The internal structure changes whether the block implements a thermal model (building climate control) or a FSM for generic appliance, as it will be presented in the next two sections. The function load_appliance.mat needs to receive in input the .csv file which contains the P-Q consumption pattern. The file is provided in the following specific format, eg.:
#DATE (ISO 8601): 20120426T151853
#LOAD: APPLIANCE - DISHWASHER
#MANUFACTURER: BLOMBERG
#PROGRAM: STANDARD
#WORKLOAD (1-FULL, 0-EMPTY): 0.5
#TAGS: TIMESTAMP(ms);P;Q
0.000000;0.000000;0.000000

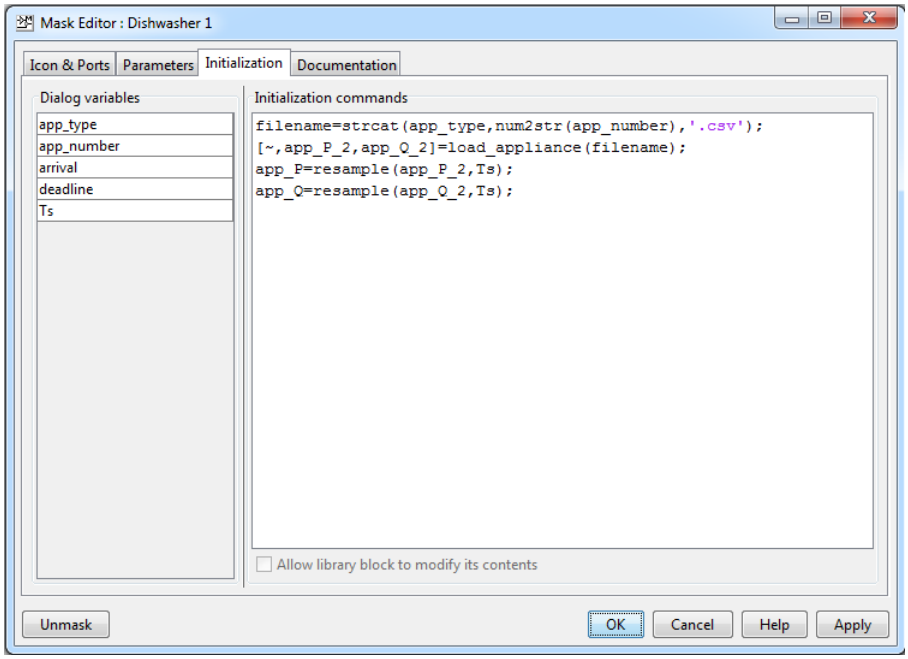

Figure 18: configuration pane of the generic appliance model: specification of a new consumption profile.

1000.000000;2.448000;0.000000
2000.000000;6.702000;0.000000
3000.000000;8.558000;0.000000
4000.000000;12.696000;5.791000
5000.000000;15.596000;13.399000
6000.000000;17.849000;19.073000
7000.000000;19.539000;23.360000
8000.000000;20.807000;26.607000
9000.000000;21.757000;28.963000
10000.000000;22.565000;30.778000
11000.000000;23.076000;32.060000

However, should the input file be in another format, it is possible to program a different function to read the file and use it in the initialization. In the following, only the multi-room model will be presented as it is more accurate for problem analysis and simulation. However, the single-room model is convenient for control design purposes, especially for predictive control, since it provides the aggregated heat demand of the entire building and, being of lower order, requires less computation effort. After the predictive controller has computed the optimal heat power to the building, this value is partialized among the heaters in the rooms with a round robin-based logic, or a more sophisticated techniques [10].

5.1 MULTI-ROOM MODEL OF POWER FLEXHOUSE

With respect to space heating and cooling, the model developed is very specific to the application, meaning that the block structure should not be modified and its parameters are set according to the results of an identification process [10], [1], [11]. In order to implement a new model for space heating and cooling, it is necessary to first define the model structure in terms of differential equations, then identify parameters from experimental data or a-priori estimation and finally implement the differential equations in a Simulink block. In order to simulate the same type of building but with slight modifications in thermal mass and insulation, it suffices to modify the C and R parameters in the script that loads the model. Moreover, by just replicating the Power FlexHouse space heating model and summing up the electrical consumption it is possible to simulate a group of analogous buildings. Randomly chosen initial conditions can be set in order to desynchronize the systems operation.

The thermal model can be interfaced with thermostatic heaters control or with more advanced predictive controllers, it suffices to modify the connections from the heating system to the rooms, as it is presented in Fig.19. The heat dynamics of Power FlexHouse is modeled with a set of coupled differential equations, each of which corresponds to a specific room. The model is presented in Eq. 6, which parameters are depicted in Tab. 2. The space heating simulation block is composed by subsystems which represent the single rooms. Figure 20 shows the inner components of the space heating block, where it is depicted the block of room 4.

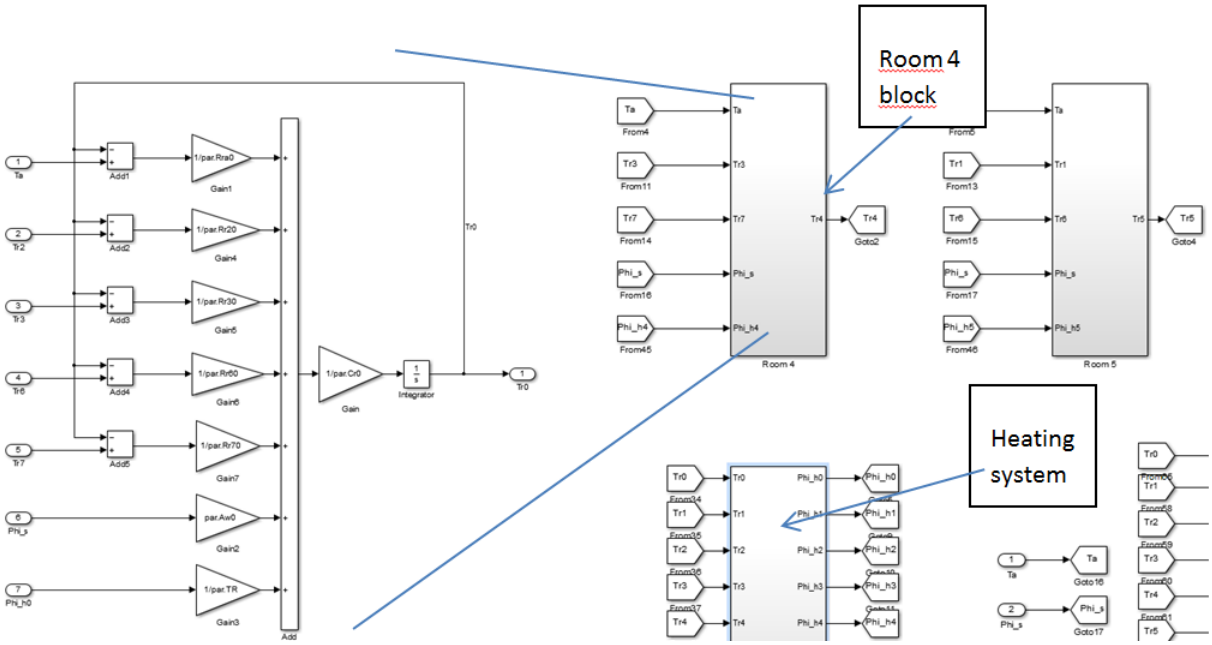

Figure 19: detail of a subsystem block modelling room heat dynamics.

Each room block receives input from the heating power provided by the respective room heater, the solar irradiation, the external temperature and the temperatures of the adjacent rooms. The output of the room block is the room temperature, which is fed to the visualization block and the heating system block for temperature control. This latter embeds the models of electric heaters and the thermostatic controllers, although it is possible to connect the heaters to a MPC controller with minor modifications in the blocks. The block of room 4 is expanded on the left side of Fig. 19. Rooms' heat dynamics are grouped in the space heating block which, together with other two models for dishwasher and microwave, is presented

below in Fig. 21.

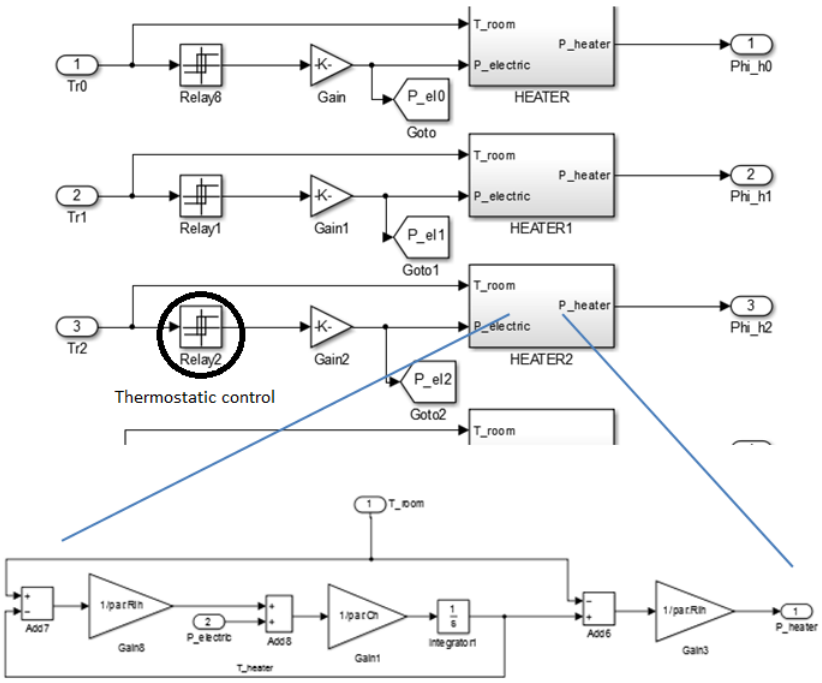

Figure 20: implementation of the heating system.

Figure 22 shows the space heating user interface, which allows choosing some simulation parameters as rooms initial temperature, thermostats upper and lower bounds, and the seed used to randomly vary equations parameters within the given statistic bounds (given Tab. 2).

The power output of each block is summed up to compute the aggregate consumption of the building. Note that it is possible to access the power consumption of each device independently. Other types of appliances such as white goods are modeled via FSM, which implementation is presented in the following section.

5.2 GENERIC APPLIANCE MODEL

Figure 23 shows FSM model implemented in each appliance block, which includes also an additional system for generating the triggering signals necessary to run the FSM chart.

Figure 24 presents the details of the FSM model in Fig. 23. The appliance FSM is composed by three concurrent state flow charts: S1, S2 and S3. S1 implements the structure proposed in Fig. 12 for device operation, while S2 is deputed to compute the task priority, as it is presented in [3]. Finally, S3 can simulate system faults.

Figure 25 presents a generic appliance block that has been specialized for a dishwasher (via the GUI in Fig. 26). The block receives in input a triggering binary signal, which starts the device when the value is one and stops the device when the value is zero. The block output is the dishwasher active and reactive power consumption.

The FSM model provides a user interface, depicted in Fig. 26, for choosing the type of appliance to simulate. By setting the arrival time and the deadline it is possible to compute the task priority factor, which can be used by a DSM system [27].

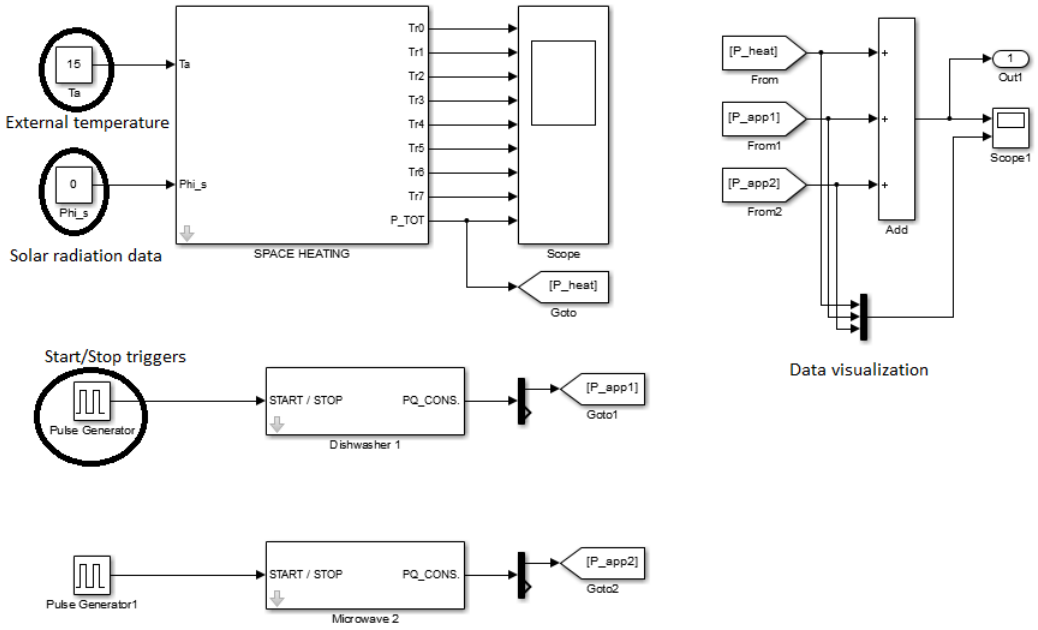

Figure 21: general schematics of building consumption simulator.

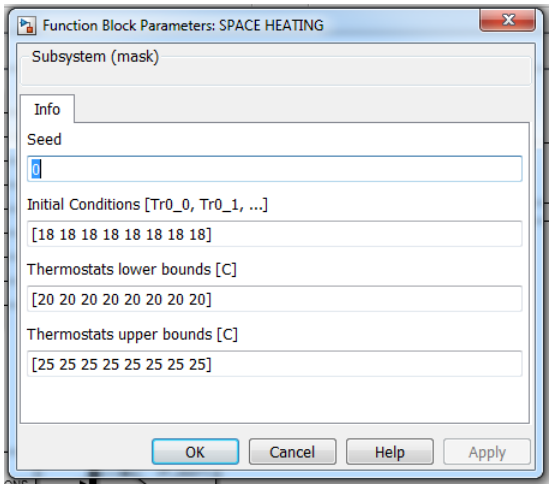

Figure 22: GUI for parameters setting in space heating block.

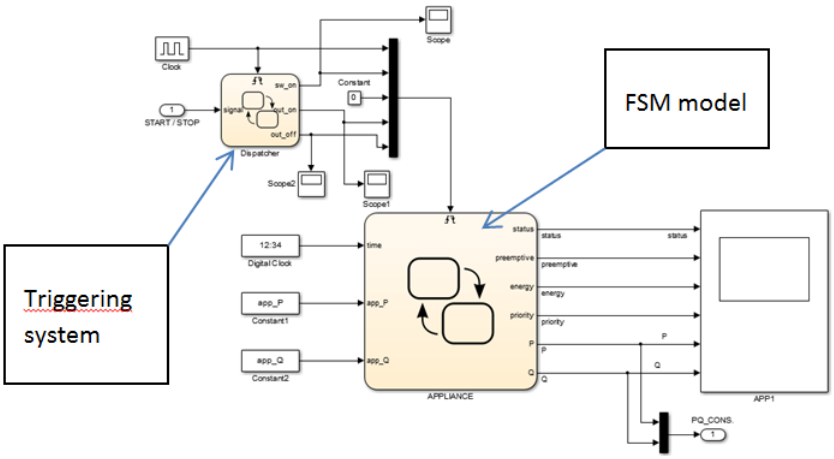

Figure 23: generic appliance FSM model and interface.

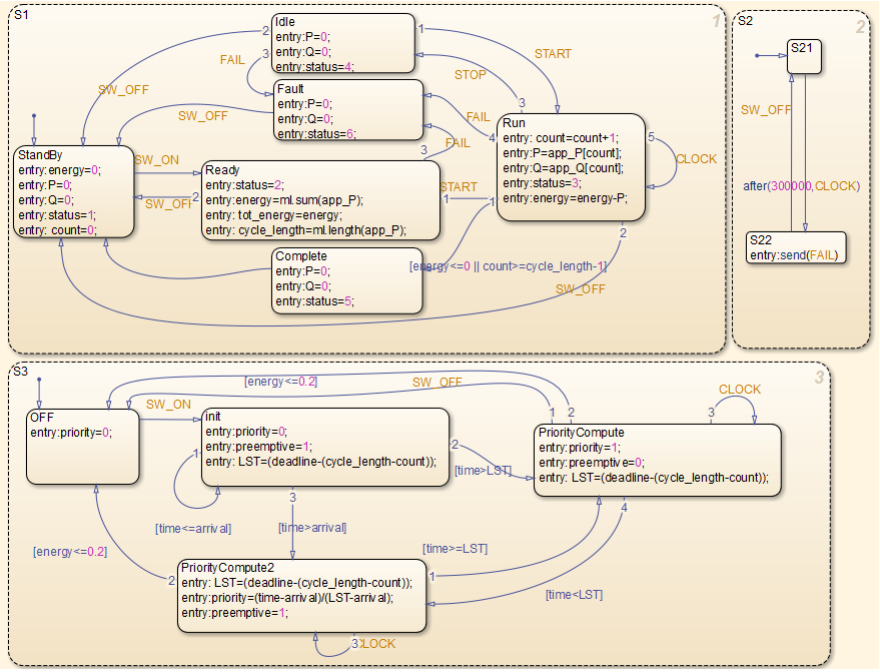

Figure 24: FSM stateflow chart.

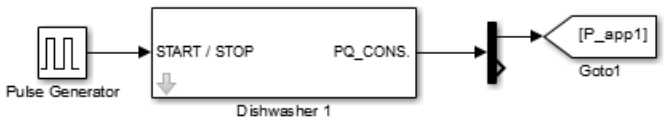

Figure 25: appliance blockset.

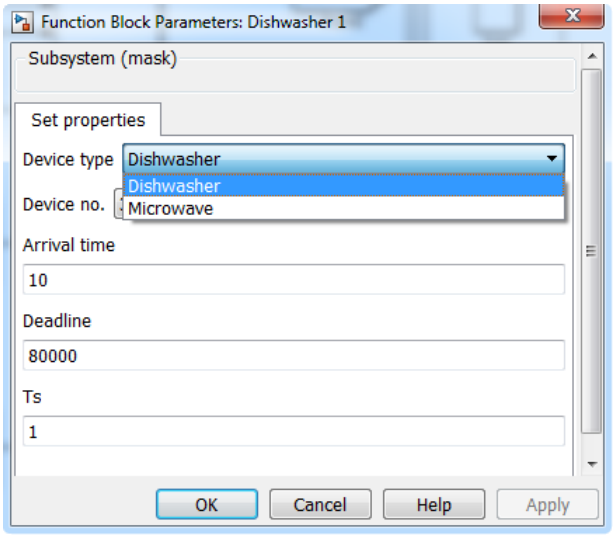

Figure 26: generic appliance GUI.

The consumption profile is averaged over a period set by the parameter *Ts*, which cannot be smaller than the sampling time of the measured appliance power profile, and it is usually equal to the time step used for the simulation.

5.3 REFRIGERATOR

The refrigerator block implements the two-states thermal model presented in Chapter 3 .

The inputs for the refrigerator model are: electric power consumption and ambient temperature, while the output is the inner temperature of the refrigeration chamber. The electric power consumption is assumed constant and equal to the average measured power consumption during a refrigeration cycle, while the ambient temperature depends on the room in which the refrigerator is placed in and is fed from the specific room block. As next development of the refrigerator model, it is foreseen a model for the compressor and the thermal dynamics of foodstuff.

5.4 SIMULATING THE TOTAL HOUSEHOLD CONSUMPTION

The following chart shows twelve hours simulation of a building energy demand, which is related to space heating, dishwasher and microwave operation. The simulation setup is depicted in Fig. 20. The dishwasher is operated every three hours, while the microwave every four hours. The upper chart shows the total consumption and the lower chart the consumption of individual devices: space heating (in yellow), dishwasher (in purple) and microwave (in light blue).

6 CONCLUSIONS

This report presents models for simulating household consumption, which can be related to the operation of such devices as electric space heaters, dishwasher, and refrigerators. The approach proposed in this study strives at catching the

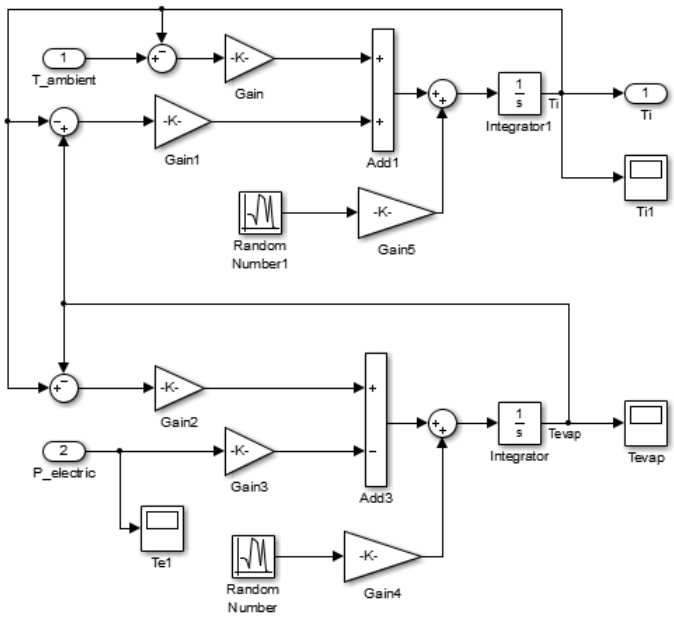

Figure 27: refrigerator T_i T_{evap} model.

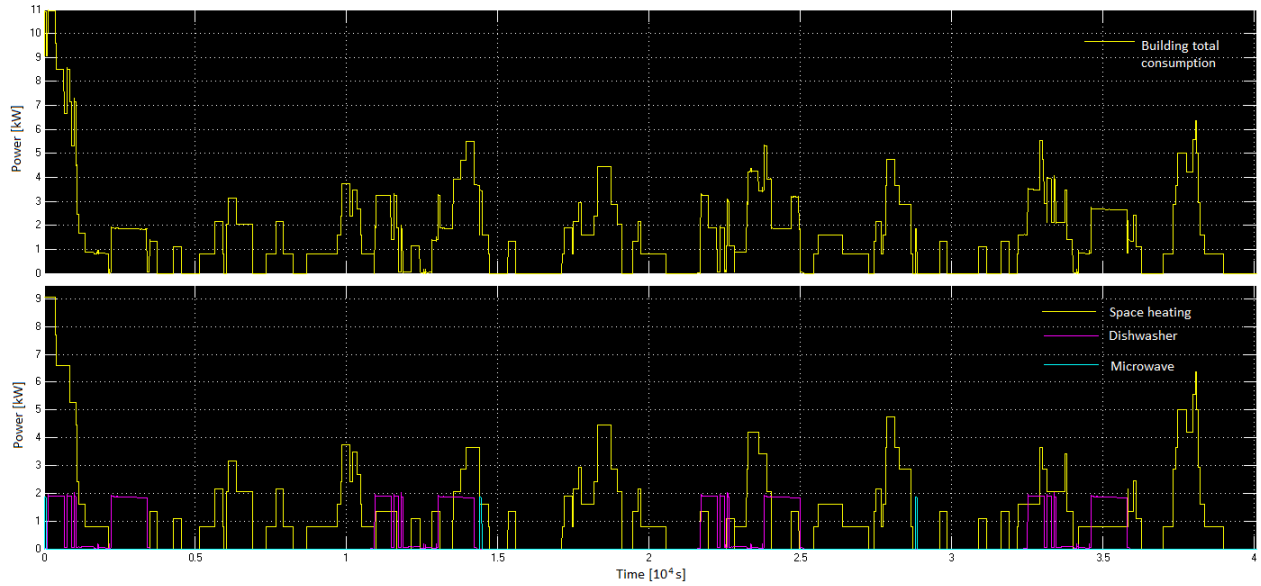

Figure 28: simulation of aggregated building consumption.

dominant dynamics associated to devices operation, which are assumed to be in the time scale of seconds.

Thanks to the flexibility of Simulink platform, the proposed framework enables to include new device models provided their thermal model or power consumption profile. Device models include interface for control, consisting of start/stop signals and output data of the specific process. Depending on the type of information needed for feedback control, models could be modified in order to output more data regarding the process. In the presented implementation, household appliances models include the necessary interface to be embedded in the DSM architecture presented in [27].

The presented appliances models can be interfaced to Simpowersystems models to study the impact of control policies for residential DSM systems. The impact on large networks can be also be investigated by interfacing Simulink with other softwares for Power Systems analysis, such as Neplan and DIgSilent Power Factory.

6 REFERENCES

[1] P. Bacher and H. Madsen, "Identifying suitable models for the heat dynamics of buildings," *Energy and Buildings*, vol. 43, no. 7, pp. 1511–1522, 2011.

[2] European Commission. (2011) Eurostat. [Online]. Available: http://epp.eurostat.ec.europa.eu/portal/page/portal/eurostat/home/

[3] A. Simon and R. Belles, "Estimated state level energy flows in 2008," Lawrence Livermore National Laboratory, Tech. Rep., 2009.

[4] Bellifemine, F.L. et al., "Smart grid: Energia & ict," *Notiziario tecnico Telecom Italia*, vol. 3, pp. pp. 15–32, Dec. 2009.

[5] iPower Consortium, "iPower Glossary," 2012.

[6] World Business Council for Sustainable Development (WBCSD), "Transforming the market: Energy efficiency in the buildings," 2009.

[7] B. Flynn and P. Energy, "Key smart grid applications," *Protection and Control Journal*, no. 8, pp. 29–34, 2009.

[8] Z. Xu, M. Gordon, M. Lind, and J. Ostergaard, "Towards a danish power system with 50% wind - smart grids activities in denmark," in *Power & Energy Society General Meeting, 2009. PES'09. IEEE*. IEEE, 2009, pp. 1–8.

[9] A. Troi. (2012, Mar.) About ipower. [Online]. Available: http://www.ipower-net.dk/About_iPower.aspx

[10] A. Thavlov, "Dynamic optimization of power consumption," Master's thesis, Technical University of Denmark, DTU, DK-2800 Kgs. Lyngby, Denmark, 2008.

[11] D. E. Morales Bondi and J. Parvizi, "Modeling, identification and control for heat dynamics of buildings using robust economic model predictive control," Master's thesis, Technical University of Denmark, DTU, DK-2800 Kgs. Lyngby, Denmark, 2012.

[12] R. Juhl, N. R. Kristensen, P. Bacher, J. Kloppenborg, and H. Madsen, "Ctsm-r user guide," *Technical University of Denmark*, vol. 2, 2013.

[13] H. Madsen and P. Thyregod, *Introduction to general and generalized linear models*. CRC Press, 2011.

[14] N. R. Kristensen, H. Madsen, and S. B. Jørgensen, "Parameter estimation in stochastic grey-box models," *Automatica*, vol. 40, no. 2, pp. 225–237, 2004.

[15] M. Baadsgaard, J. Nielsen, H. Spliid, H. Madsen, and M. Preisel, "Estimation in stochastic differential equations with a state dependent diffusion term," in *SYSID*, 1997.

[16] H. Madsen, *Time series analysis*. CRC Press, 2008, vol. 72.

[17] H. Joseph Newton, *Statistics 626, lectures notes*. Texas A&M University, 1999.

[18] A. Rabl, "Parameter estimation in buildings: methods for dynamic analysis of measured energy use," *Journal of Solar Energy Engineering*, vol. 110, no. 1, pp. 52–66, 1988.

[19] R. C. Sonderegger, "Dynamic models of house heating based on equivalent thermal parameters," Ph.D. dissertation, 1978.

[20] H. Boyer, J. Chabriat, B. Grondin-Perez, C. Tourrand, and J. Brau, "Thermal building simulation and computer generation of nodal models," *Building and Environment*, vol. 31, no. 3, pp. 207 – 214, 1996.

[21] J. Bloem, *System identification applied to building performance data*. Office for Official Publications of the European Communities, 1994.

[22] A. Thavlov and H. Madsen, "A stochastic model for an office building with air infiltration," *Preprint submitted to Elsevier*, 2013.

[23] C. J. Hermes and C. Melo, "Assessment of the energy performance of household refrigerators via dynamic simulation," *Applied Thermal Engineering*, vol. 29, no. 5Ã¢âĆňâĂIJ6, pp. 1153 – 1165, 2009.

[24] C. J. Hermes, C. Melo, F. T. Knabben, and J. M. GonÃČÂğalves, "Prediction of the energy consumption of household refrigerators and freezers via steady-state simulation," *Applied Energy*, vol. 86, no. 7Ã¢âĆňâĂIJ8, pp. 1311 – 1319, 2009.

[25] J. Gupta, M. R. Gopal, and S. Chakraborty, "Modeling of a domestic frost-free refrigerator," *International Journal of Refrigeration*, vol. 30, no. 2, pp. 311 – 322, 2007.

[26] G. T. Costanzo, P. Bacher, M. Marinelli, F. Sossan, and H. Madsen, "Grey-box modeling for system identification of household refrigerators: a step toward smart appliances," in *4th IEEE International Youth Conference on Energy (IYCE)*, June 2013.

[27] G. T. Costanzo, G. Zhu, M. F. Anjos, and G. Savard, "A system architecture for autonomous demand side load management in smart buildings," *Smart Grid, IEEE Transactions on*, vol. 3, no. 4, pp. 2157–2165, 2012.

